

## Supporting Information

### Highly Selective Hydrogenolysis of Lignin $\beta$ -O-4 Models by Coupled Polyoxometalates/CdS Photocatalytic System

Mo Zhang<sup>a,b,†</sup>, Zheng Li<sup>a,†</sup>, Yeqin Feng<sup>a</sup>, Xing Xin<sup>a</sup>, Guo-Yu Yang<sup>a\*</sup>, Hongjin Lv<sup>a\*</sup>

<sup>a</sup> MOE Key Laboratory of Cluster Science, Beijing Key Laboratory of Photoelectroic/Electrophotonic Conversion Materials, School of Chemistry and Chemical Engineering, Beijing Institute of Technology, Beijing 102488, P. R. China.

<sup>b</sup> School of Pharmacy, Key Laboratory of Innovative Drug Development and Evaluation, Hebei Medical University, Shijiazhuang 050017, P. R. China.

\*Corresponding author e-mail: [hlv@bit.edu.cn](mailto:hlv@bit.edu.cn); [ygy@bit.edu.cn](mailto:ygy@bit.edu.cn)

†These authors contributed equally to this work.

## Table of Contents

<b>Fig. S1</b> TEM images of the CdS QDs	S3
<b>Fig. S2</b> Digital photos of the reaction solution using different capping agent QDs	S3
<b>Fig. S3</b> UV-vis spectra of CdS QDs with different capping agents	S4
<b>Fig. S4</b> XPS spectra of CdS QDs	S5
<b>Fig. S5</b> Polyhedral and ball-and-stick representations of polyoxometalates: <b>Ni<sub>4</sub>P<sub>2</sub></b> and <b>Ni<sub>9</sub>P<sub>3</sub></b>	S6
<b>Fig. S6</b> FT-IR spectra of <b>Ni<sub>4</sub>P<sub>2</sub></b> and <b>Ni<sub>9</sub>P<sub>3</sub></b>	S6
<b>Fig. S7</b> UV-vis spectra of <b>Ni<sub>9</sub>P<sub>3</sub></b> and <b>Ni<sub>4</sub>P<sub>2</sub></b> catalyst with the same concentration	S7
<b>Fig. S8</b> Digital photos of the reaction solution before and after photocatalysis	S7
<b>Fig. S9</b> SEM and corresponding elemental mapping images of isolated CdS-MPA QDs	S8
<b>Fig. S10</b> High resolution XPS spectra of isolated CdS-MPA QDs from NiCl <sub>2</sub> -catalyzed	S8
<b>Fig. S11</b> UV-vis spectra of CdS-MPA QDs before and after photocatalysis	S9
<b>Fig. S12</b> Photocatalytic hydrogenolysis of PP-one	S9
<b>Fig. S13</b> Gas chromatography (GC) from the photocatalytic hydrogenolysis of PP-one	S10
<b>Fig. S14</b> Energy level diagram and cyclic voltammogram	S10
<b>Fig. S15</b> Gas chromatography (GC) trace of hydrogen gas	S11
<b>Table S1</b> Semiconductor photocatalysts for lignin conversion	S12
<b>Table S2</b> Screening of reaction conditions for photocatalytic hydrogenolysis of PP-one	S13
<b>Fig. S16</b> <sup>1</sup> H NMR and <sup>13</sup> C NMR spectra of compound <b>1a</b>	S14
<b>Fig. S17</b> <sup>1</sup> H NMR and <sup>13</sup> C NMR spectra of compound <b>2a</b>	S15
<b>Fig. S18</b> <sup>1</sup> H NMR and <sup>13</sup> C NMR spectra of compound <b>3a</b>	S16
<b>Fig. S19</b> <sup>1</sup> H NMR and <sup>13</sup> C NMR spectra of compound <b>4a</b>	S17
<b>Fig. S20</b> <sup>1</sup> H NMR and <sup>13</sup> C NMR spectra of compound <b>5a</b>	S18
<b>Fig. S21</b> <sup>1</sup> H NMR and <sup>13</sup> C NMR spectra of compound <b>6a</b>	S19
<b>Fig. S22</b> The structure and GC-MS spectra of compound <b>7a</b>	S20

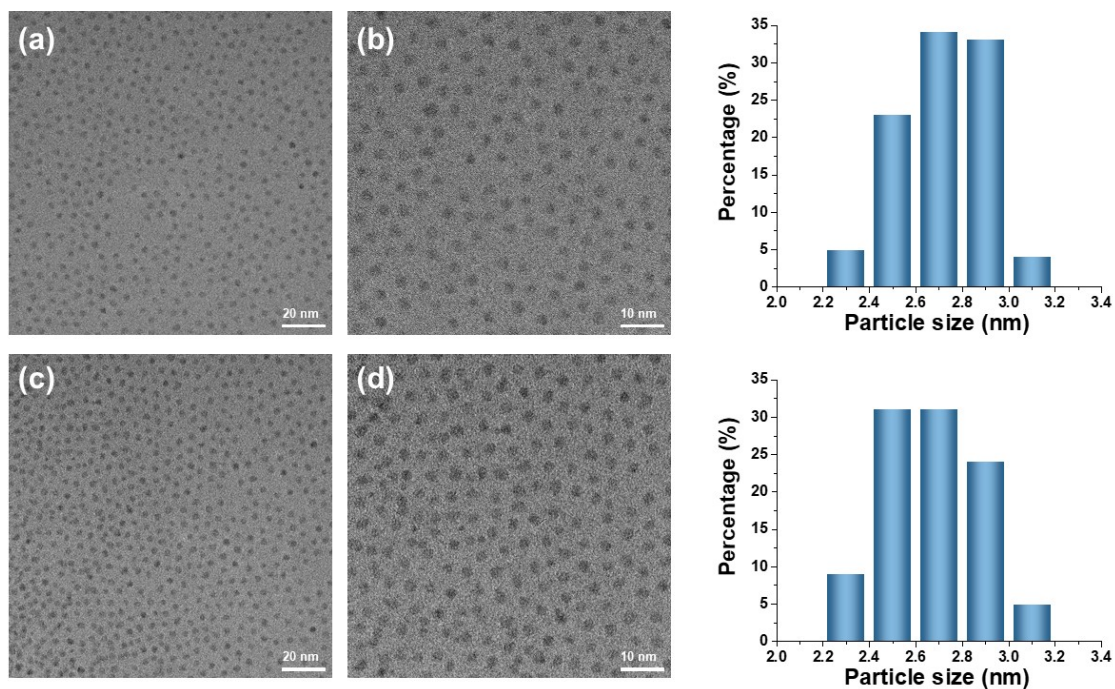


**Fig. S1** TEM images (scale bars: (a) 20 nm and (b) 10 nm, respectively) of CdS-OA QDs, the average length was calculated to be 2.73 nm; (scale bars: (c) 20 nm and (d) 10 nm, respectively) of CdS-MPA QDs, the average length was calculated to be 2.66 nm. It was noticed that ligand exchange does almost not affect the size of CdS QDs

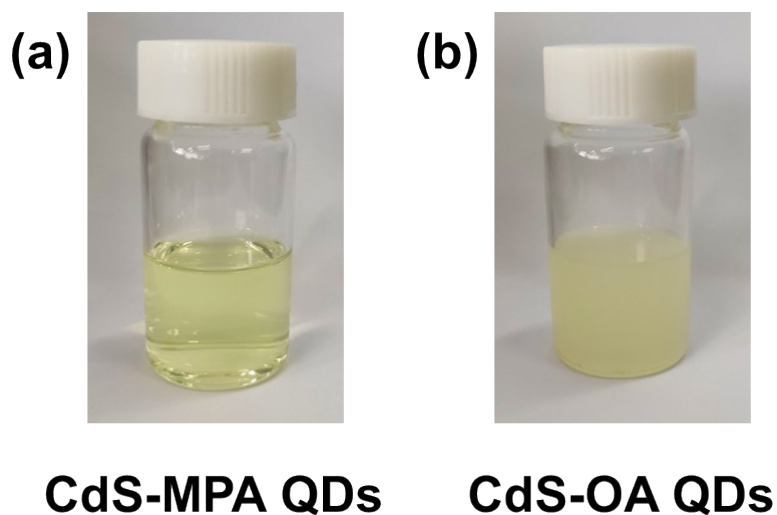


**Fig. S2** Digital photos of the reaction solution using different capping agent QDs: (a) CdS-MPA QDs and (b) CdS-OA QDs

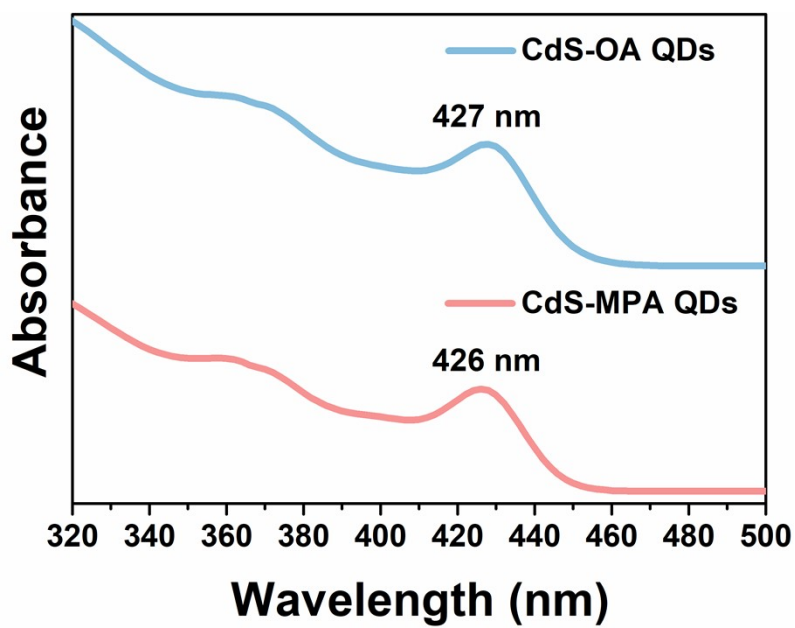


**Fig. S3** UV-vis spectra of CdS QDs with different capping agents. Note: the spectrum of OA-CdS was measured in hexane, while the spectra of MPA-CdS samples were measured in water

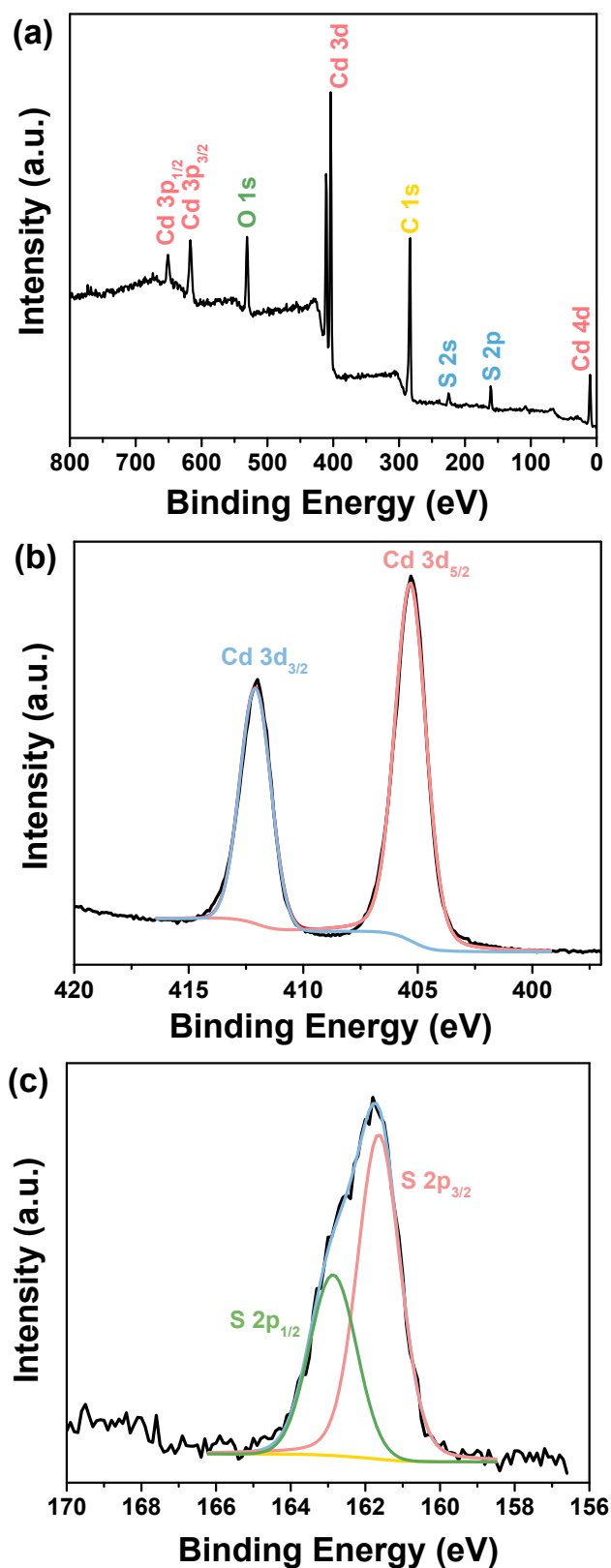


**Fig. S4** (a) The survey XPS spectra of CdS-MPA QDs, and corresponding high resolution XPS signals of (b) Cd 3d, (c) S 2p

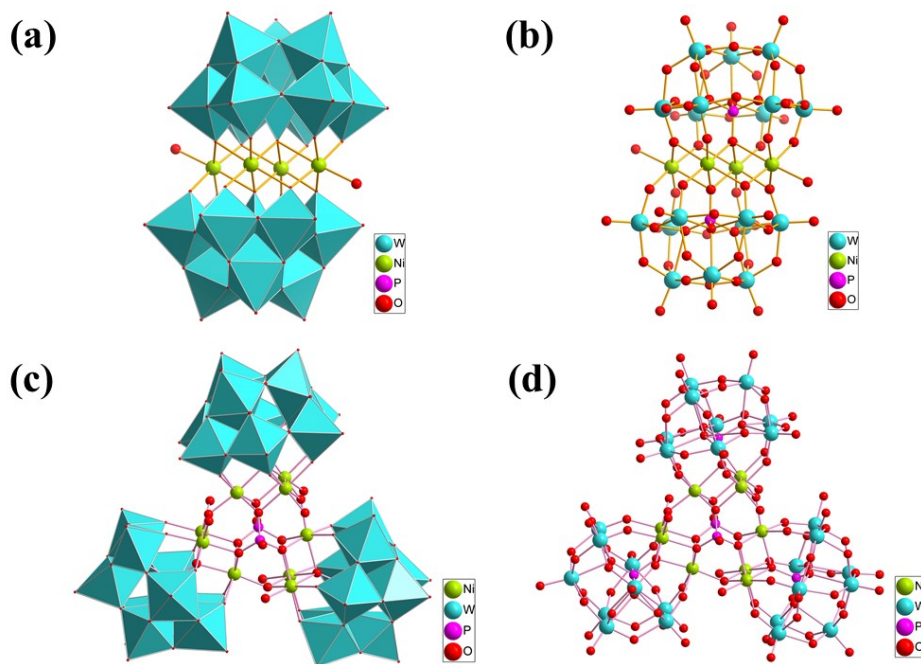


**Fig. S5** Polyhedral and ball-and-stick representations of two polyoxometalates: (a-b)  $\text{Ni}_4\text{P}_2$  and (c-d)  $\text{Ni}_9\text{P}_3$

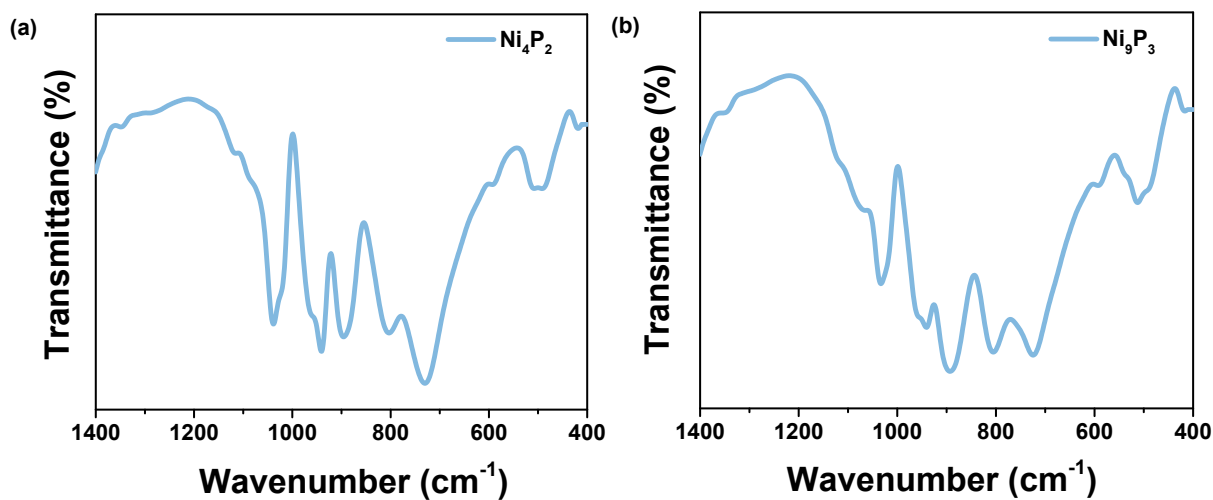


**Fig. S6** FT-IR spectra of (a)  $\text{Ni}_4\text{P}_2$ , (b)  $\text{Ni}_9\text{P}_3$ , ~ 2 wt % in KBr

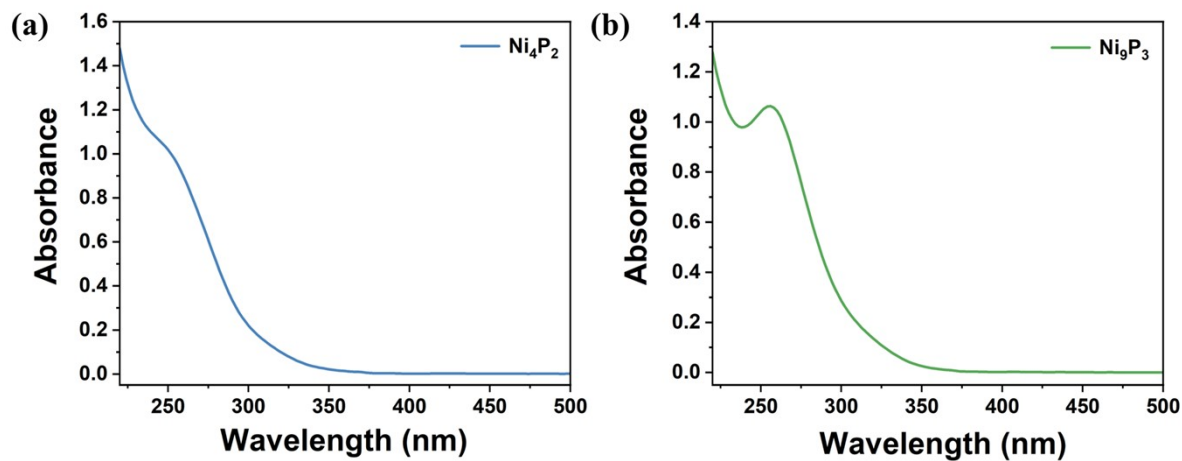


**Fig. S7** UV-vis spectra of  $\text{Ni}_9\text{P}_3$  and  $\text{Ni}_4\text{P}_2$  catalyst at the same concentration (0.0016 mM)

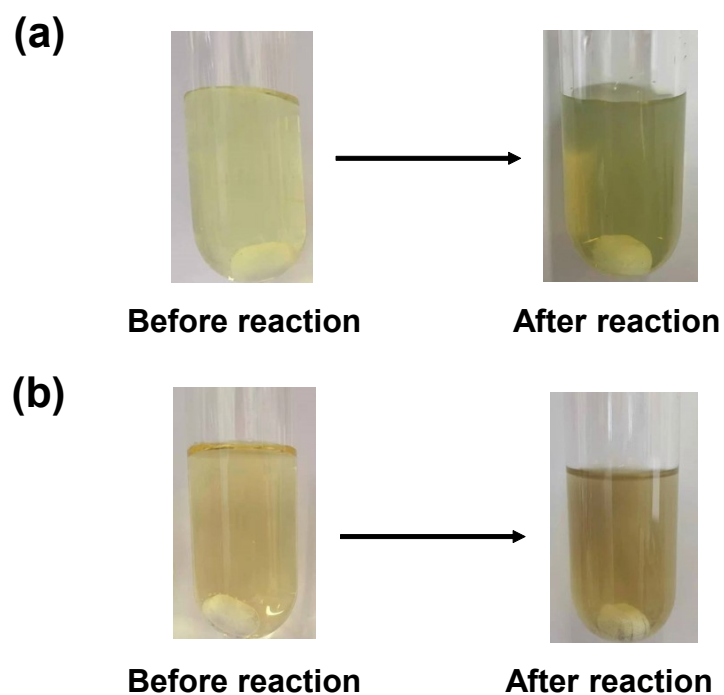


**Fig. S8** Digital photos of the reaction solution before and after photocatalysis using (a) 0.1 mM of  $\text{Ni}_9\text{P}_3$  catalyst and (b) 0.9 mM of  $\text{NiCl}_2$ . Reaction conditions: 10 mM of PP-one (**1a**), 1  $\mu\text{M}$  of CdS-MPA QDs, 10 mL of iso-propanol/ $\text{H}_2\text{O}$  (3/2), blue LED (450 nm), 8h, Ar/ $\text{CH}_4$  (4/1) atmosphere

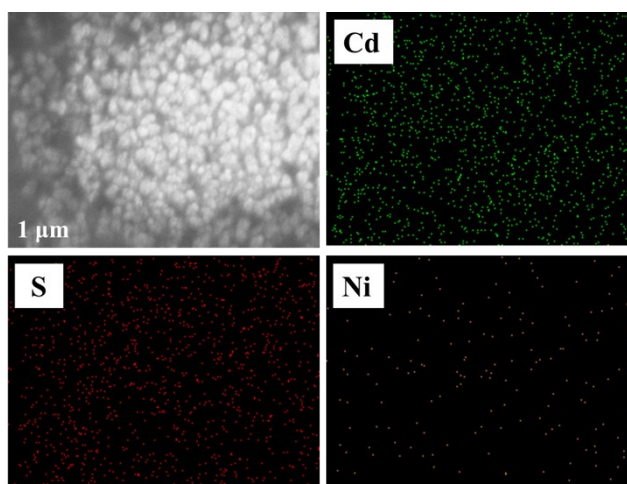


**Fig. S9** SEM and corresponding elemental mapping images of isolated CdS-MPA QDs from NiCl<sub>2</sub>-catalyzed post-reaction solution. Reaction conditions: 10 mM of PP-one (**1a**), 1 μM of CdS-MPA QDs, 10 mL of iso-propanol/H<sub>2</sub>O (3/2), blue LED (450 nm), 8h, Ar/CH<sub>4</sub> (4/1) atmosphere

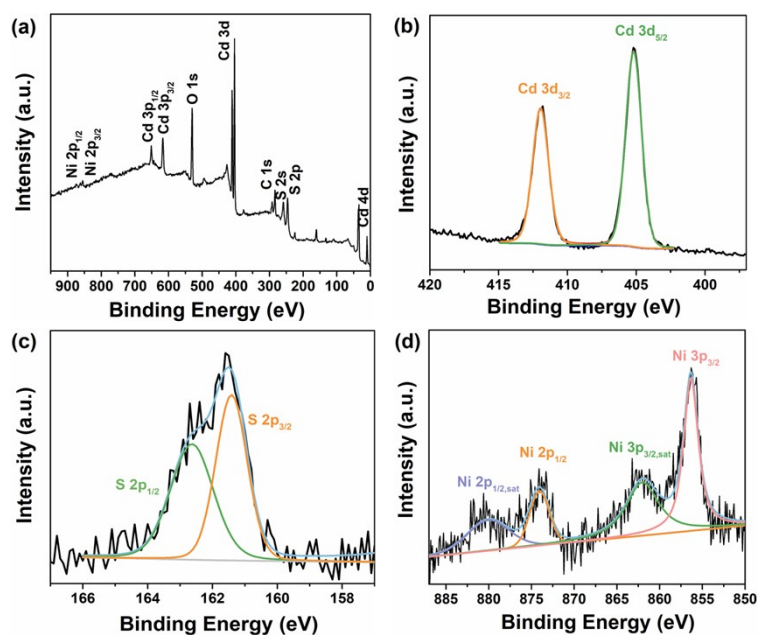


**Fig. S10** High resolution XPS spectra of (a) Full XPS spectrum, (b) Cd 3d, (c) S 2p, and (d) Ni 2p signals of isolated CdS-MPA QDs from NiCl<sub>2</sub>-catalyzed post-reaction solution after photocatalysis for 8 h



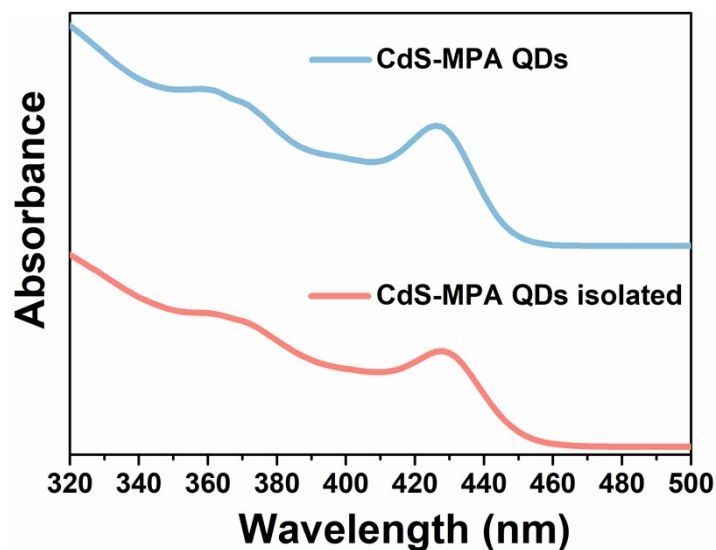


**Fig. S11** UV-vis spectra of CdS-MPA QDs before and after photocatalysis

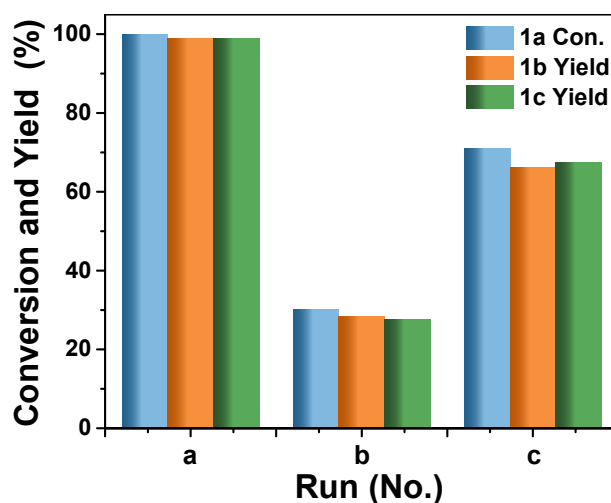


**Fig. S12** Photocatalytic hydrogenolysis of PP-one. (a) the first run using fresh CdS-MPA QDs and  $\text{Ni}_9\text{P}_3$  catalyst, (b) the second run using isolated CdS-MPA QDs and no fresh  $\text{Ni}_9\text{P}_3$  catalyst was added in this cycle, (c) the third run using isolated CdS-MPA QDs and fresh  $\text{Ni}_9\text{P}_3$  catalyst. Standard reaction conditions: 10 mM of PP-one (**1a**), 1  $\mu\text{M}$  of CdS-MPA QDs, 0.1 mM of  $\text{Ni}_9\text{P}_3$  catalyst, 10mL of iso-propanol/ $\text{H}_2\text{O}$  (3/2), blue LED (450 nm), 8h, Ar/ $\text{CH}_4$  (4/1) atmosphere

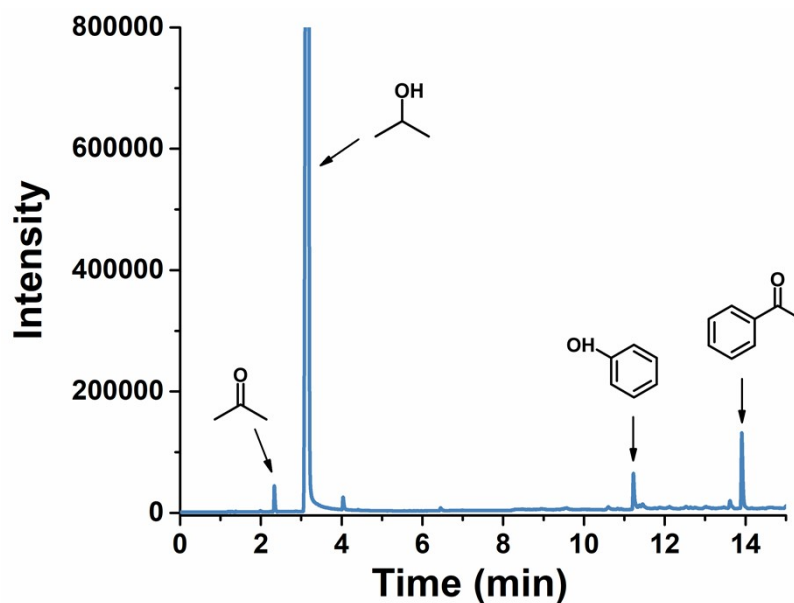


**Fig. S13** Gas chromatography (GC) from the photocatalytic hydrogenolysis of PP-one. Reaction conditions: 10 mM of PP-one (1a), 1  $\mu$ M of CdS-MPA QDs, 0.1 mM of  $\text{Ni}_9\text{P}_3$ , 10mL of iso-propanol/ $\text{H}_2\text{O}$  (3/2), blue LED (450 nm), 8h, Ar/ $\text{CH}_4$  (4/1) atmosphere

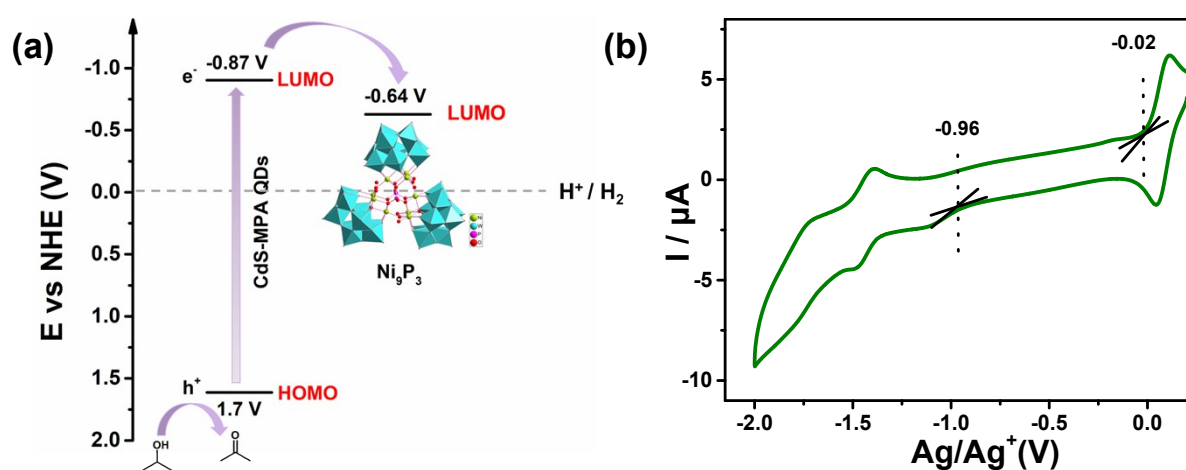
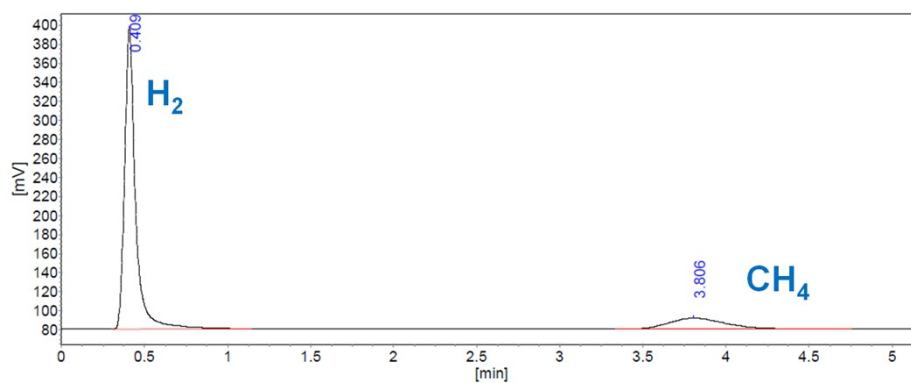


**Fig. S14** (a) Schematic energy level diagram for photocatalytic hydrogenolysis of PP-one; (b) Cyclic voltammogram of  $\text{Ni}_9\text{P}_3$  (0.1 mM) in 0.1 M TBAPF<sub>6</sub> and 0.01M AgNO<sub>3</sub> acetonitrile solution using glassy carbon working electrode, Ag/Ag<sup>+</sup> reference electrode, and Pt silk counter electrode; Scan rate: 100 mV/s. The measured potential was expressed by converting to normal hydrogen electrode (NHE)



**Analysis result table**

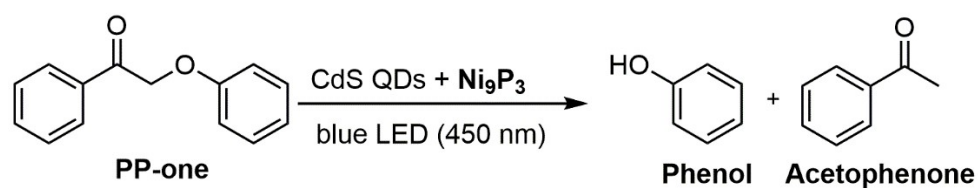
Entry	Retention time (min)	Peak height (uV)	Peak area (uV*s)	Area percentage %
1	0.409	315679	1438574	83.0850
2	3.806	11702	292874	16.9150

**Fig. S15** Gas chromatography (GC) trace of hydrogen gas produced from the photocatalytic hydrogenolysis of PP-one. Reaction conditions: 10 mM of PP-one (**1a**), 1  $\mu$ M of CdS-MPA QDs, 0.1 mM of  $\text{Ni}_9\text{P}_3$ , 10mL of iso-propanol/ $\text{H}_2\text{O}$  (3/2), blue LED (450 nm), 8h, Ar/ $\text{CH}_4$  (4/1) atmosphere

**Table S1 Semiconductor Photocatalysts for Lignin Conversion**

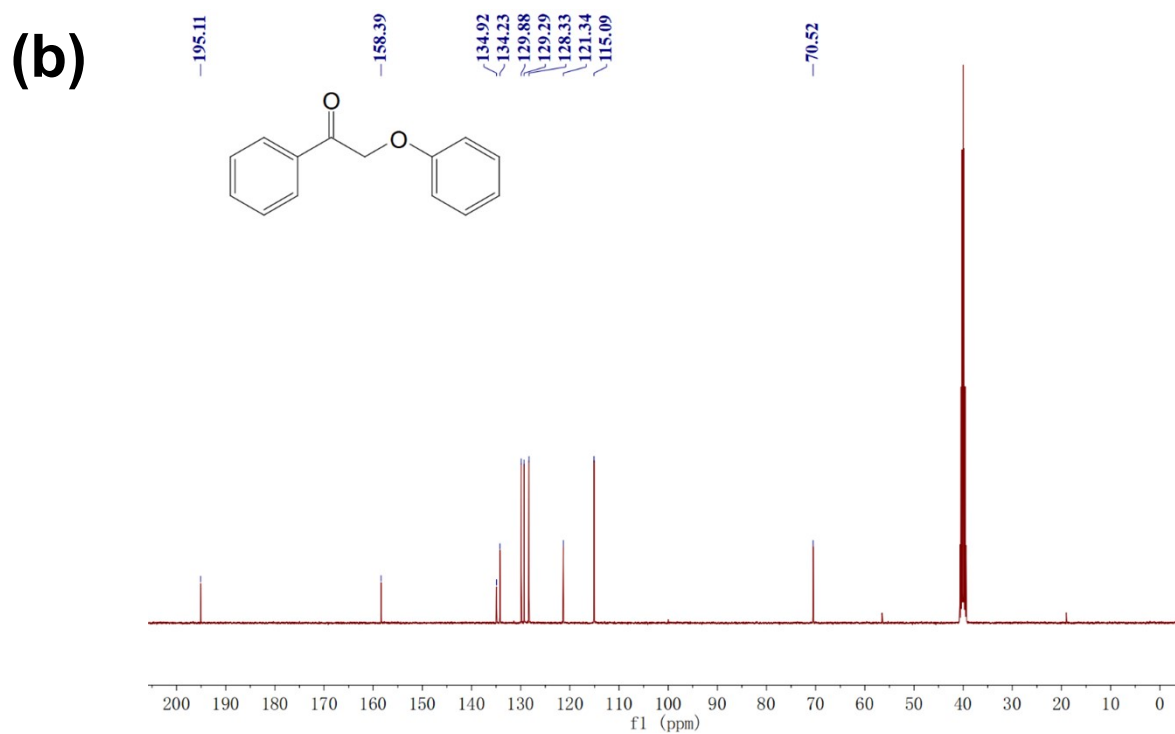
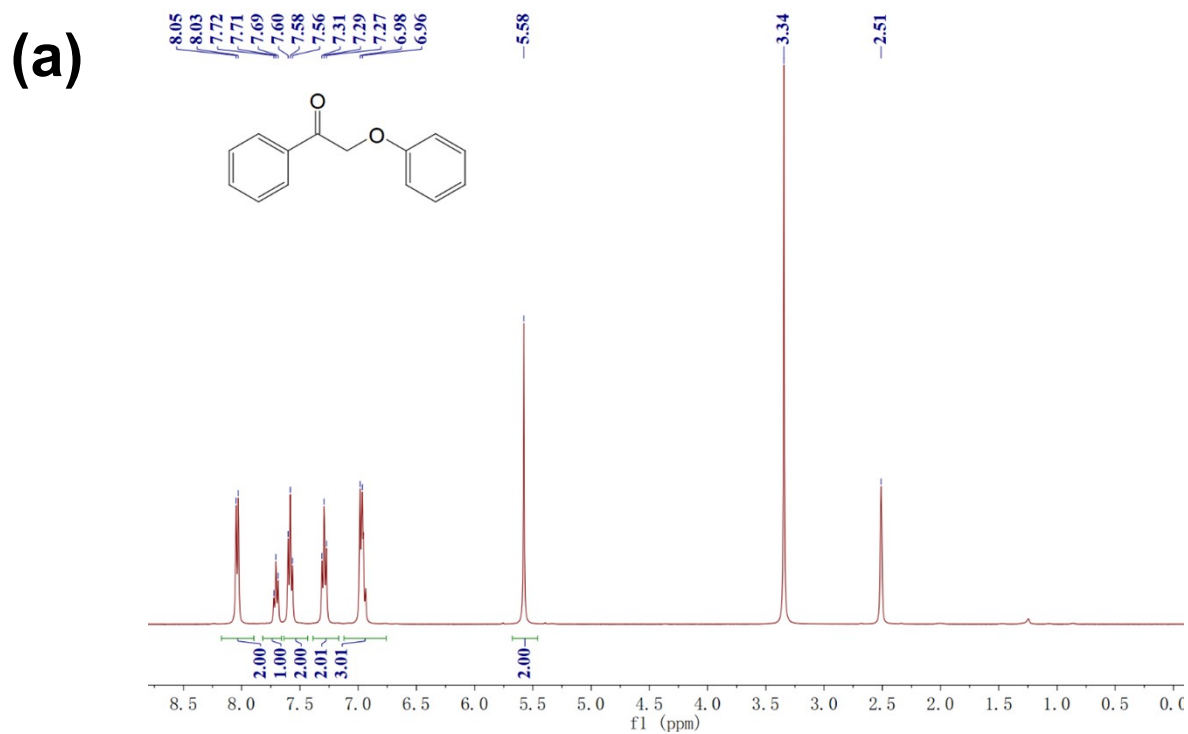
Entry	Catalyst	Heterogeneous/Homogeneous	Substrate concentration	Reaction time	Product	Conv. [%]	Yield [%]	Ref.
1	CdS-MPA QDs (1 $\mu$ M) + Ni <sub>9</sub> P <sub>3</sub> (0.1 mM)	Homogeneous	10 mM	8 h	A: phenol, B: acetophenone	99	A: 99 B: 99	This work
2	ZnIn <sub>2</sub> S <sub>4</sub> (5 mg)	Heterogeneous	100 mM	4 h	A: phenol, B: acetophenone, C: benzyl phenyl ether	99	A: 83 B: 90 C: 6	4
3	Ni/CdS (20 mg)	Heterogeneous	5 mM	8 h	A: phenol, B: acetophenone	100	A: 99 B: 99	9
4	CdS (10mg)	Heterogeneous	20 mM	3 h	A: phenol, B: acetophenone	99	A: 93 B: 91	37
5	Pb/ZnIn <sub>2</sub> S <sub>4</sub> (10 mg), TiO <sub>2</sub> (5 mg)	Heterogeneous	133 mM	33 h	A: phenol, B: acetophenone	94	A: 94 B: 76	50
6	Zn <sub>4</sub> In <sub>2</sub> S <sub>7</sub> (10 mg)	Heterogeneous	20 mM	4 h	A: phenol, B: acetophenone, C: benzyl phenyl ether	99	A: 82 B: 86 C: 10	51
7	Mesoporous g-C <sub>3</sub> N <sub>4</sub> (10 mg)	Heterogeneous	50 mM	10 h	A: acetophenone, B: benzaldehyde, C: benzoic acid	96	A: 51 B: 30 C: 21	54
8	In <sub>2</sub> S <sub>3</sub> (20 mg)	Heterogeneous	0.16 mM	8.384 min	C: 2-methoxy-4-hydroxybenzaldehyde	N.A.	N.A.	55
9	Zn <sub>4</sub> In <sub>2</sub> S <sub>7</sub> (10mg)	Heterogeneous	20 mM	2 h	A: phenol, B: acetophenone, C: benzyl phenyl ether	93	A: 70 B: 51 C: 17	56
10	Cd <sub>x</sub> Zn <sub>1-x</sub> S (10 mg)	Heterogeneous	20 mM	2 h	A: phenol, B: acetophenone	93	A: 85 B: 36	57
11	Ligand-controlled CdS QDs (15 mg)	Heterogeneous	Native lignin	8 h	Aromatic monomers	27	N.A.	58

**Table S2 Screening of Reaction Conditions for Photocatalytic Hydrogenolysis of PP-one<sup>a</sup>**

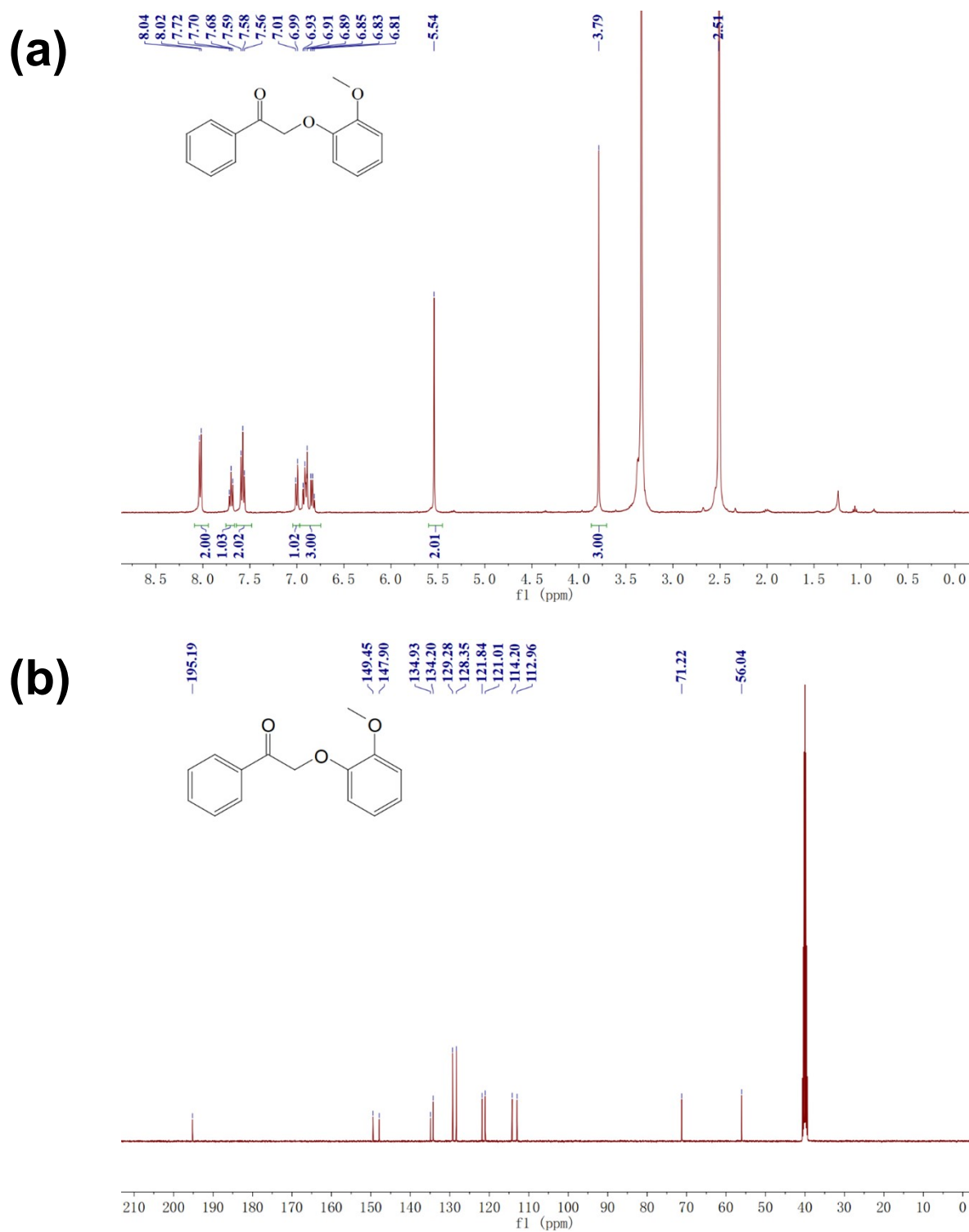


Entry	Conv. (%)	Product Yield (%)		H <sub>2</sub> (μmol)	Acetone (μmol)
		Phenol	Acetophenone		
1	99.3	99.3	98.8	142.3	205.3
2 <sup>b</sup>	0	0	0	0	78.4
3 <sup>c</sup>	48.5	48.4	43.1	17.9	76.7
4 <sup>d</sup>	43.5	42.8	21.8	405.2	276.3

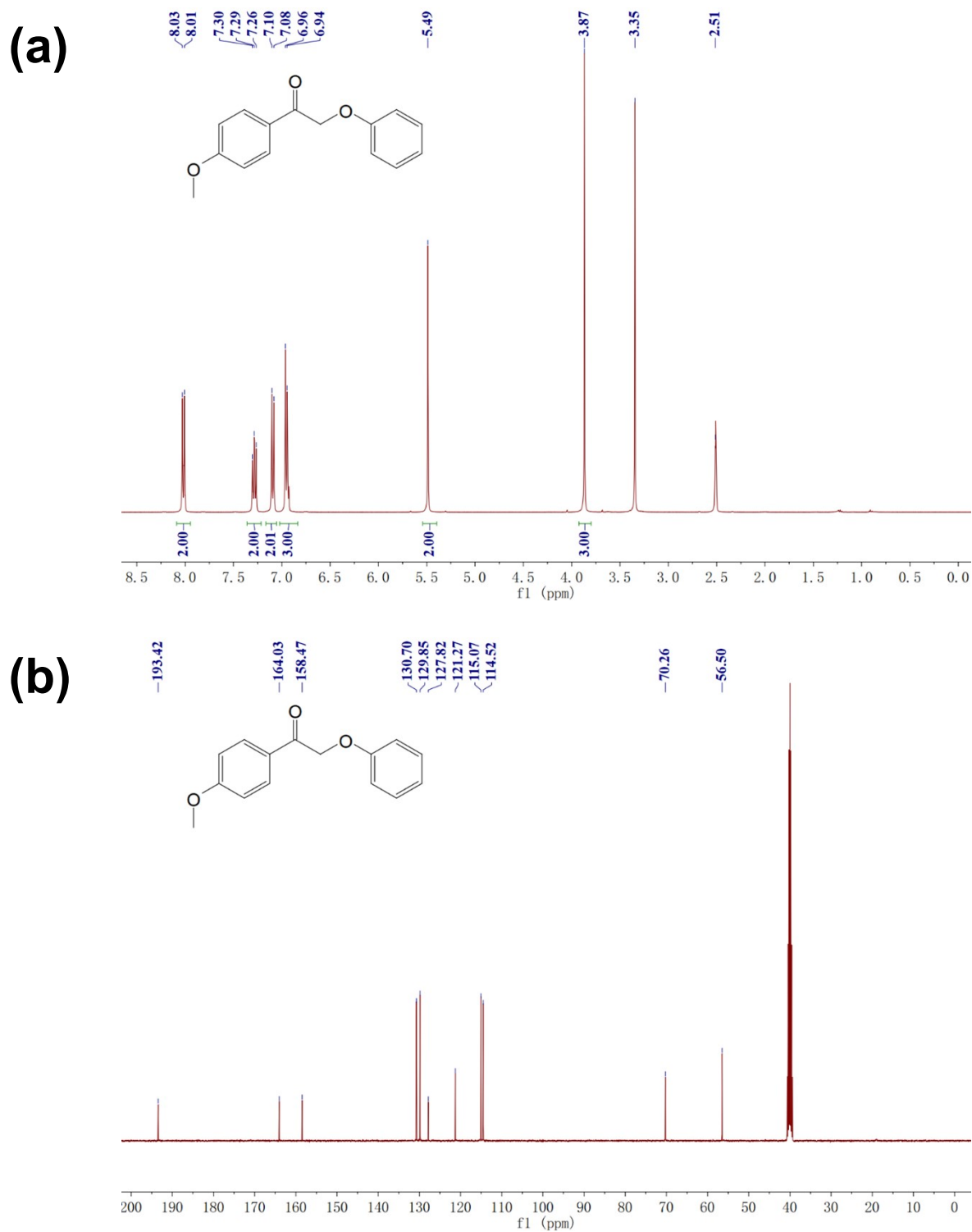
<sup>a</sup> Reaction conditions: 10mM of 2-phenoxy-1-phenylethan-1-one, 1 μM of CdS-MPA QDs, 0.1 mM of Ni<sub>9</sub>P<sub>3</sub>, 10 mL of isopropanol/H<sub>2</sub>O (3/2), blue LED (450 nm), Ar/CH<sub>4</sub> (4/1) atmosphere, 8 h. <sup>b</sup> with 10mM K<sub>2</sub>S<sub>2</sub>O<sub>8</sub>. <sup>c</sup> with 10mM Na<sub>2</sub>C<sub>2</sub>O<sub>4</sub>. <sup>d</sup> with 2 wt % Pt



**Fig. S16** (a)  $^1\text{H}$  NMR spectra and (b)  $^{13}\text{C}$  NMR spectra of compound 2-phenoxy-1-phenylethan-1-one (**1a**)



**Fig. S17** (a)  $^1\text{H}$  NMR spectra and (b)  $^{13}\text{C}$  NMR spectra of compound 2-(2-methoxyphenoxy)-1-phenylethan-1-on (**2a**)





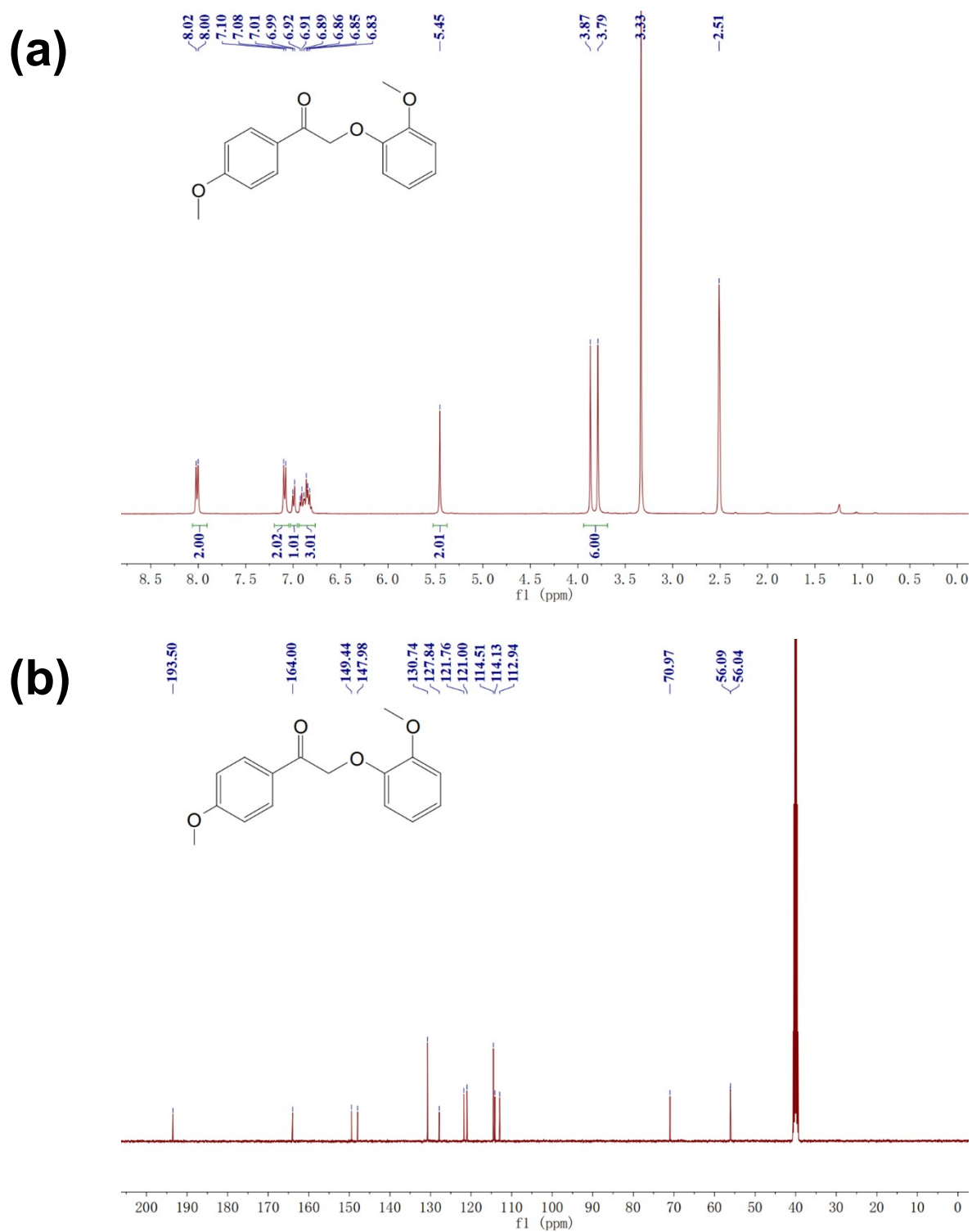
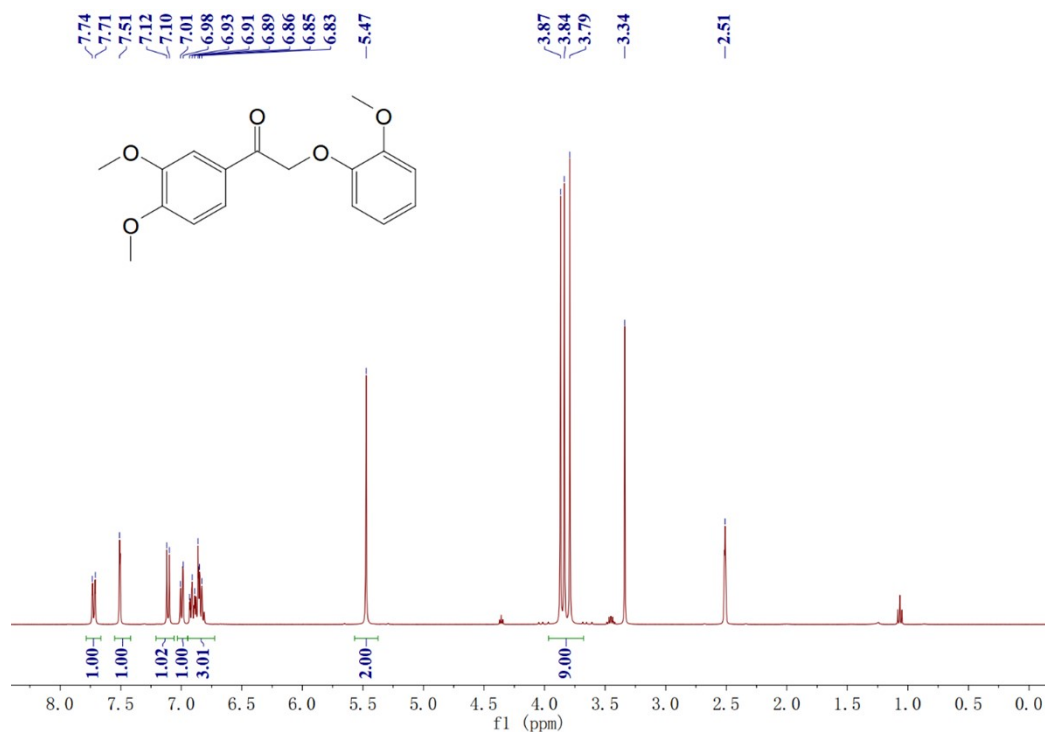


**Fig. S19** (a)  $^1\text{H}$  NMR spectra and (b)  $^{13}\text{C}$  NMR spectra of compound 2-(2-methoxyphenoxy)-1-(4-methoxyphenyl)ethan-1-one (**4a**)

(a)



(b)

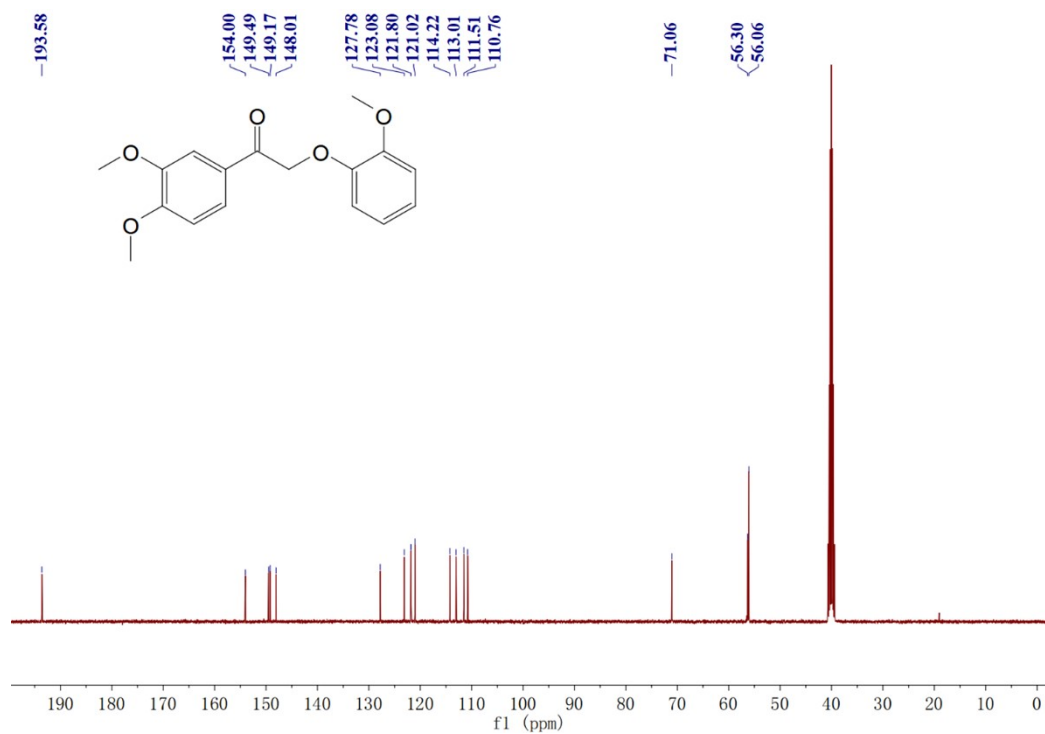


**Fig. S20** (a) <sup>1</sup>H NMR spectra and (b) <sup>13</sup>C NMR spectra of compound 1-(3,4-dimethoxyphenyl)-2-(2-methoxyphenoxy)ethan-1-one (**5a**)

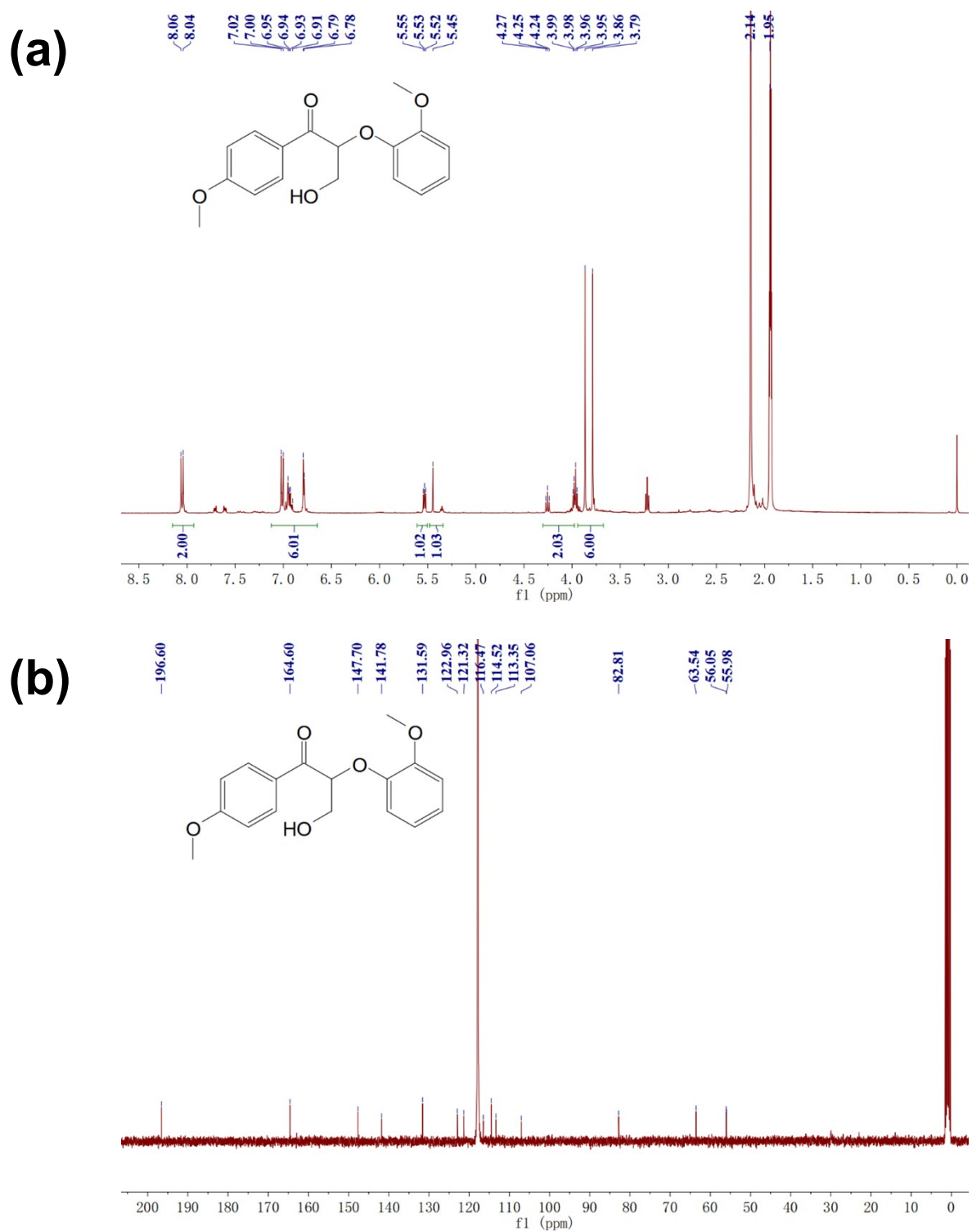


**Fig. S21** (a)  $^1\text{H}$  NMR spectra and (b)  $^{13}\text{C}$  NMR spectra of compound 3-hydroxy-2-(2-methoxyphenoxy)-1-(4-methoxyphenyl)propan-1-one (**6a**)

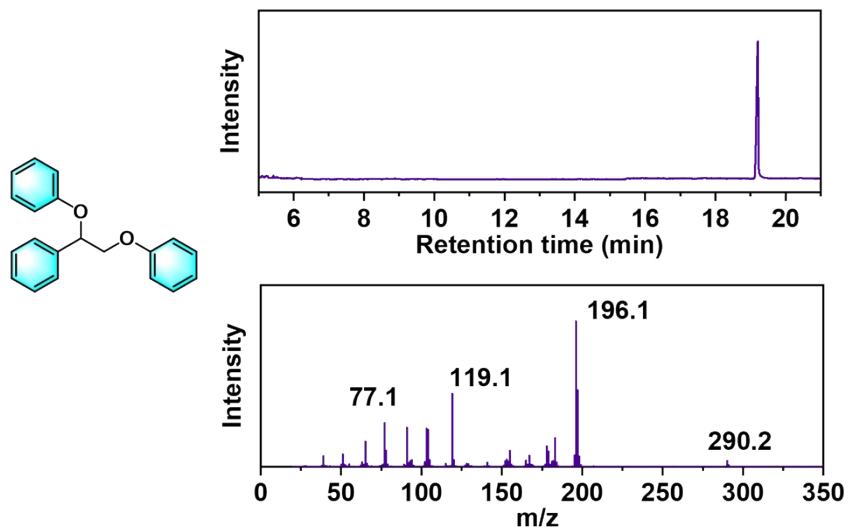


**Fig. S22** The structure and GC-MS spectra of compound ((1-phenylethane-1,2-diyl)bis(oxy))dibenzene (**7a**)